

Article

Control Mechanism of Microbial Degradation on the Physical Properties of a Coal Reservoir

Daping Xia ^{1,2}, Pengtao Gu ³, Zhenhong Chen ^{4,*}, Linyong Chen ⁵, Guoqin Wei ⁵, Zhenzhi Wang ¹, Song Cheng ⁶ and Yawei Zhang ³

¹ Institute of Resources and Environment, Henan Polytechnic University, Jiaozuo 454003, China

² Collaborative Innovation Center of Coal Work Safety and Clean High Efficiency Utilization, Jiaozuo 454000, China

³ School of Energy Science and Engineering, Henan Polytechnic University, Jiaozuo 454000, China

⁴ Research Institute of Petroleum Exploration & Development, Beijing 100083, China

⁵ State Key Laboratory of Coal and Coalbed Methane Co Mining, Jincheng 048000, China

⁶ College of Chemistry and Chemical Engineering, Henan Polytechnic University, Jiaozuo 454003, China

* Correspondence: cbmjimcoco@126.com

Abstract: This study addressed the effect of microbial methane production on the physical properties of a coal reservoir. Two kinds of coal samples before and after anaerobic degradation were tested by a low-temperature liquid nitrogen adsorption test and an isothermal adsorption and diffusion coefficient test. The influence of the characteristics of microbial gas production on the coal physical properties was analyzed. Due to the differences in the physical properties of the coal samples, the effect of microbial production is different. Coal is a macromolecular organic compound, mainly aromatic and lignin derivatives, containing carbon and nitrogen sources that can be used by microorganisms. Microorganisms secrete extracellular enzymes to decompose covalent bonds and functional groups of macromolecules in coal and eventually produce methane, which will change the physical properties of coal. It was found that microbial anaerobic degradation could increase the content of coalbed methane, change the pore structure of coal, reduce the fractal dimension of the coal surface and smooth the coal surface. At the same time, microbial degradation has changed the physical properties of coal reservoirs to some extent, increased the diffusion of coal reservoirs and improved the pore connectivity of coal reservoirs, which provides more of a scientific basis for the development of coalbed methane.

Keywords: microbial yield; coal pore structure; diffusion; pore connectivity; dual effect



Citation: Xia, D.; Gu, P.; Chen, Z.; Chen, L.; Wei, G.; Wang, Z.; Cheng, S.; Zhang, Y. Control Mechanism of Microbial Degradation on the Physical Properties of a Coal Reservoir. *Processes* **2023**, *11*, 1347. <https://doi.org/10.3390/pr11051347>

Academic Editors: Maria Alice Zarur Coelho, Ailton Cesar Lemes and Filipe Smith Buarque

Received: 27 March 2023

Revised: 20 April 2023

Accepted: 21 April 2023

Published: 27 April 2023



Copyright: © 2023 by the authors. Licensee MDPI, Basel, Switzerland. This article is an open access article distributed under the terms and conditions of the Creative Commons Attribution (CC BY) license (<https://creativecommons.org/licenses/by/4.0/>).

1. Introduction

Coal Bed Methane (CBM) is mainly adsorbed on the surface of coal matrix particles. CBM transport is influenced by a combination of factors, such as the composition of the coal itself, its pore characteristics and its diffusivity [1–3]. The reason for the low rate of coalbed methane extraction and utilization is the poorly developed network of pore fractures of the coal reservoir. This paper examines the effect of microbial action on the physical properties of coal reservoirs. Most CBM wells can produce significant volumes of gas by relying on hydraulic fracturing techniques. However, the same technology used to increase production in Chinese CBM wells is very ineffective [4–6]. This can be attributed to the variability of coal grades, permeability and geological conditions or to the performance of the fracturing fluid. In any case, the CBM production increase is not satisfactory [7]. With the emergence of multiple gas displacement technology, the principle of methane replacement by injecting gas into a coal seam becomes applicable [8–10]. In terms of coal reservoirs in China, if only the CO₂ displacement effect is relied upon to improve the CBM recovery rate, without considering increasing the CO₂ injection pressure, this process has

a negative effect on permeability due to the formation of new fractures in the coal seam, which cause the coal matrix to swell [11–16].

Hence, the abovementioned CBM enhancement technologies are still insufficient, but CBM promises to be an important addition to clean and efficient energy sources. In response, the Microbial Enhancement Coalbed Methane (MECBM) technology has been developed. This technology works mainly by injecting methanogens and nutrients into a coal seam. Microbial degradation is used to achieve increased CBM production [17–19]. At present, the technology, after comprehensive study from multiple viewpoints, has formed the basis of the initial implementation of Coalbed Gas Bioengineering (CGB) in this system. In the system engineering aspect of increasing coalbed methane production, coal matrix porosity studies form a key part of coal reservoir modification. The biotransformation of coal has been shown to lead to a significant expansion of the coal matrix. In residual coal, the width of $<5\ \mu\text{m}$ pores and fissures decreases markedly [20]. However, some studies have shown that the microbial action of the coal increases the surface of coal fissures [21–23]. The influence of microorganisms on the physical properties of reservoirs has not been conclusively established. It is unknown whether coal seams that have undergone biological action are conducive to increased CBM content.

This study used lignite and bituminous coal as substrates. The original flora of the coal seam in mine water were taken as the enrichment object. Microbial anaerobic degradation experiments were then conducted. Pore connectivity before and after coal degradation was characterized by the low-temperature liquid nitrogen adsorption–desorption curve. The variation in a series of parameters such as the pore size distribution characteristics was determined by isothermal adsorption, permeability and diffusion coefficient tests. These experiments served to study the changes in the desorption and diffusion capacity of coal reservoirs after microbial action, to reveal the mechanism of coal reservoir modification after microbial degradation and to provide a reference for the application of microbial production enhancement technology.

2. Materials and Methods

2.1. Experimental Design

2.1.1. Preparation of Coal Samples

The coal samples are low-rank lignite (HM) from the Baiyinhua Coal Mine in Inner Mongolia Autonomous Region and medium-rank bituminous coal (JM) from the Shaqu Coal Mine in Liulin County, Shanxi Province. Mine water samples were taken from the deep mine water of the Guhanshan Mine in Jiaozuo City, Henan Province, also in China. The pore system and physical parameters of the collected coal samples before and after degradation were systematically analyzed. First, two core columns approximately 25 mm in diameter were drilled from each of the two coal rock samples. The remaining block samples were then used to make coal rock slices and to perform coal vitrinite reflectance measurements. Finally, the electromagnetic ore crusher was used to crush the coal, and pulverized coal with a particle size of 80~100 mesh was screened. There will be more consumption in the process of grinding into 80~100 mesh pulverized coal. In this experiment, a set of a blank group and two experimental groups was set up. The experimental group was 500 mL bacterial solution + 50 g HM or JM pulverized coal, plus two parallel samples. The parallel sample was also set up to be 500 mL bacterial solution + 50 g HM or JM pulverized coal, and another was 500 mL bacterial solution + core column. That is, a coal sample in this batch of experiments requires about 50 g of coal pillars and 150 g of 80~100 mesh pulverized coal, totaling 200 g. According to the GB/T 30732-2014 and GB/T 31391-2015 national standards, industrial and elemental analysis of the coal samples was performed. Table 1 shows the test results. The remaining coal samples are stored at 105 °C in an electrothermal constant temperature blast dryer.

Table 1. Proximate analysis, ultimate analysis and maximum vitrinite reflectance of coal samples.

Coal Sample Number	Proximate Analysis (%)			Ultimate Analysis (%)				R^o_{max} (%)
	M_{ad}	A_{ad}	V_{daf}	C_{daf}	H_{daf}	$(O+S)_{daf}$	N_{daf}	
HM	15.10	7.74	44.40	69.91	6.27	22.08	1.74	0.46
JM	0.44	11.44	17.08	87.69	4.95	5.94	1.42	1.53

2.1.2. Enrichment Culture of Bacteria

Laboratory enrichment culture medium was used to enrich the microorganisms in mine water. Methanogenic enrichment culture medium contained an organic carbon source, organic nitrogen source and other nutrients necessary for microbial growth and metabolism, including an organic carbon source: sodium formate, 2.0 g/L; sodium acetate, 2.0 g/L. Organic nitrogen source: yeast extract, 1.0 g/L; tryptone, 0.1 g/L. Inorganic salt: NH_4Cl , 1.0 g/L; $MgCl_2 \cdot 6H_2O$, 0.1 g/L; $NaHCO_3$, 2.0 g/L. pH buffer: $K_2HPO_4 \cdot 3H_2O$, 0.4 g/L; KH_2PO_4 , 0.2 g/L. Reducing agent: Na_2S , 0.2 g/L; l-cysteine hydrochloride, 0.5 g/L. Trace element liquid, 10 mL/L; vitamin solution, 10 mL/L. Composition of trace element solution: aminotriacetic acid, 1.5 g/L; $MnSO_4 \cdot 2H_2O$, 0.5 g/L; $MgSO_4 \cdot 7H_2O$, 3.0 g/L; $FeSO_4 \cdot 7H_2O$, 0.1 g/L; $NaCl$, 1.0 g/L; $CoCl_2 \cdot 6H_2O$, 0.1 g/L; $CaCl_2 \cdot 2H_2O$, 0.1 g/L; $CuSO_4 \cdot 5H_2O$, 0.01 g/L; $ZnSO_4 \cdot 7H_2O$, 0.1 g/L; H_3BO_3 , 0.01 g/L; $KAl(SO_4)_2$, 0.01 g/L; $NiCl_2 \cdot 6H_2O$, 0.02 g/L; $NaMoO_4$, 0.01 g/L; Deionized water, 1000 mL. Vitamin liquid composition: biotin, 2 mg/L; folic acid, 2 mg/L; b6, 10 mg/L; b2, 5 mg/L; b1, 5 mg/L; niacin, 5 mg/L; calcium pantothenate, 5 mg/L; b12, 0.1 g/L; p-aminobenzoic acid, 5 mg/L; sulfuric acid, 5 mg/L; deionized water, 1000 mL. The above drugs are weighed by an electronic balance, weighing gram-level drugs accurately to two decimal places and weighing milligram-level drugs accurately to four decimal places. The GL224-1SCN electronic balance precision was 0.0001 g.

The weighed medium was placed in a high-pressure sterilization pot and quickly moved into an anaerobic workstation after sterilization. After cooling to room temperature, adding a suitable amount of mine water, fully mixing and shaking and filling high-purity helium for 5~10 min, the bacteria liquid reached the anaerobic environment. The rubber plug was quickly plugged after inflation and the bottle mouth was sealed with sealing film; the whole process was carried out in the anaerobic workstation. After sealing, the conical flask was placed in a constant temperature incubator at 35 °C for 10–15 days. During the period, the gas was collected, and the enrichment effect was evaluated according to the methane production. If methane was not detected, it was re-enriched until methane was generated; among them, the blank control group did not produce gas.

2.1.3. Fermentation Gas Production Experiment

After successful enrichment, the enriched bacterial liquid was expanded according to the ratio of enriched bacterial liquid to medium 1:10 (at this time, the medium was replaced with an equal amount of distilled water, and the pH was adjusted to 7.0 ± 0.05). The bacteria were expanded for 10 days, and then the coal-to-biomethane experiment was carried out. According to the ratio of coal sample (g): bacteria liquid (mL) = 1:10 [24], 50 g of the coal sample was placed in a sterilized 500 mL conical flask, and 500 mL of bacteria liquid was added in the anaerobic workstation. After fully mixing, oxygen was discharged, sealed and connected to the collection bag. The gas production experiment was carried out in a constant temperature incubator at 35 °C until there was no obvious gas production. This batch of experiments was set to three groups. The first group was a blank control group with three bottles of 500 mL bacterial solution without pulverized coal. The second group was the HM group with three bottles of 500 mL bacterial solution + 50 g HM pulverized coal (two bottles were parallel) and one bottle of 500 mL bacterial solution + HM core column. The third group was the JM group with three bottles of 500 mL bacterial solution + 50 g JM pulverized coal (two bottles were parallel) and one bottle of 500 mL bacterial solution + JM core column. The first group was the blank control of the second and third groups, and the second and third groups were compared with each other. Gas samples were tested

every three days. To ensure the reproducibility of the experimental results, multiple sets of parallel samples were set up. A low-temperature liquid nitrogen adsorption test and a methane isothermal adsorption test of coal and rock were carried out before and after fermentation. The conventional porosity and permeability analysis and methane diffusion test of coal and rock were carried out before and after microbial degradation.

2.2. Test Methods

2.2.1. Low-Temperature Liquid Nitrogen Adsorption Tests

The low-temperature liquid nitrogen adsorption experiment was carried out by using a JW-BK112 automatic specific surface area pore size distribution tester. Before the test, the coal sample needs to be vacuum degassed, and the heating rate is 1.0 °C/min. The temperature is raised to 105 °C, and the constant temperature is 5 h. The test environment pressure is vacuumed down to 0.25 Pa. During the formal test, the test gas was high-purity nitrogen and high-purity helium with a concentration of 99.999%. The inlet pressure should be controlled at 0.1 MPa and 77.35 K. The coal samples were tested with liquid nitrogen as the adsorption medium, and the adsorption/desorption isotherms were obtained in the range of 0.01–0.995. To ensure the accuracy of the experiment, in principle, the sample volume does not exceed two-thirds of the total volume of the sample warehouse. The effective range of the pore size was 0.35–500 nm. BET multi-layer adsorption theory and BJH and HK/SF models were used to obtain the specific surface area, pore volume and average pore size of the coal samples.

2.2.2. Isothermal Adsorption

Using the IS-300 (Terra Tek, Salt Lake City, UT, USA) isothermal sorption instrument according to the “High-pressure isothermal adsorption test method for coal” (GB/T19560-2008) standard, isothermal adsorption tests were performed on coal before and after degradation. The maximum pressure was set to 10 MPa, and 10 pressure points were used with each pressure to reach the adsorption equilibrium.

2.2.3. Diffusion Coefficient Test

The TK-I coal-bed (shale) gas diffusion coefficient measuring instrument was used. In preparation for testing, the coal was dried and evacuated to remove pore water and residual gases. The operating current was 200 mA, the operating pressure was 25 MPa, the temperature was 120 °C ± 0.5 °C and the ring pressure was ≤ 35 MPa.

3. Experimental Results and Discussion

3.1. Output Characteristics of Biomethane

Figure 1 shows the gas production characteristics of lignite (HM) and bituminous coal (JM). The experimental results demonstrate that both HM and JM can be degraded and utilized by microorganisms, but HM was utilized to a greater extent than JM. The cumulative methane yield of HM was 152.11 µmol/g. The peak of gas production (65.05 µmol/g) was reached on the ninth day. JM coal was more difficult to degrade than HM due to its particular structure, which resulted in a longer-duration hydrolysis phase. Overall gas production lagged behind HM. Peak gas production from JM occurred on day 12, with a peak of 40.49 µmol/g and a cumulative methane production of 80.57 µmol/g.

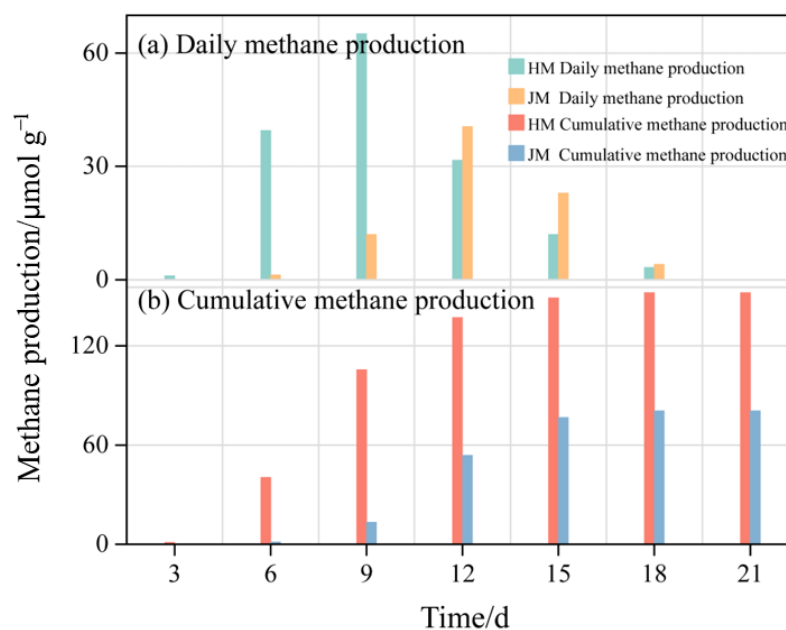


Figure 1. Biomethane production characteristics of lignite (HM) and bituminous coal (JM). (a) Daily methane production of lignite and bituminous coal. (b) Cumulative methane production of lignite and bituminous coal.

3.2. Characteristics of the Pore Structure

3.2.1. Characterization of the Coal Pore Structure

The pore structure of coal can be specifically described by testing parameters such as the pore specific surface area, total pore volume, pore size distribution and fractal dimension. The pore structure of the coal samples before and after gas production was tested by low-temperature liquid nitrogen adsorption; Figure 2 shows the corresponding nitrogen adsorption/desorption isotherms. According to the characteristics of the adsorption isotherm curves, the isothermal adsorption line could be divided into six types. The experimental results provided the liquid nitrogen adsorption curves before and after gas production from the coal samples, which had type I and type II curves of the BET classification scheme. Lignite raw coal (HM raw coal) had a type I curve. In the low-pressure region, the adsorption capacity increased rapidly, the micropores were more developed, and the sample was dominated by cylindrical micropores closed at one end. The adsorption and desorption curves of the whole process coincided closely, and their pore connectivity was good. Finally, in the high-pressure zone, adsorption increased rapidly, and capillary condensation occurred in the mesopores. Lignite residual coal (HM residual coal) had a type II curve. The adsorption and desorption curves basically coincided, and the pores were mainly slit-shaped and one-end closed cylindrical. The reason for this was that the pore capillary coalescence and the relative pressure of water evaporation from the pores appeared to be equal, resulting essentially in an overlap of the sorption and desorption curves [25].

The bituminous raw coal (JM raw coal) and bituminous residual coal (JM residual coal) had Type II curves. The adsorption and desorption curves coincided within the low-pressure and high-pressure zones, demonstrating the presence of many semi-closed and permeable pores (open) within the JM [26]. Capillary coalescence occurred mainly at relative pressures from 0.5 to 1.0. The adsorption capacity in low- and medium-pressure areas increased slowly, the interaction between coal and nitrogen was weak and the connectivity of micropores and mesopores was poor. The desorption curve had almost no hysteresis loop, indicating the presence of a closed cylindrical hole at one end. In the high-pressure region, the adsorption of both coal samples increased significantly; the development of

mesopores and good pore connectivity suggested that the pores in this type of coal still consisted mainly of parallel plate-like pores or wedge-shaped pores closed on one side.

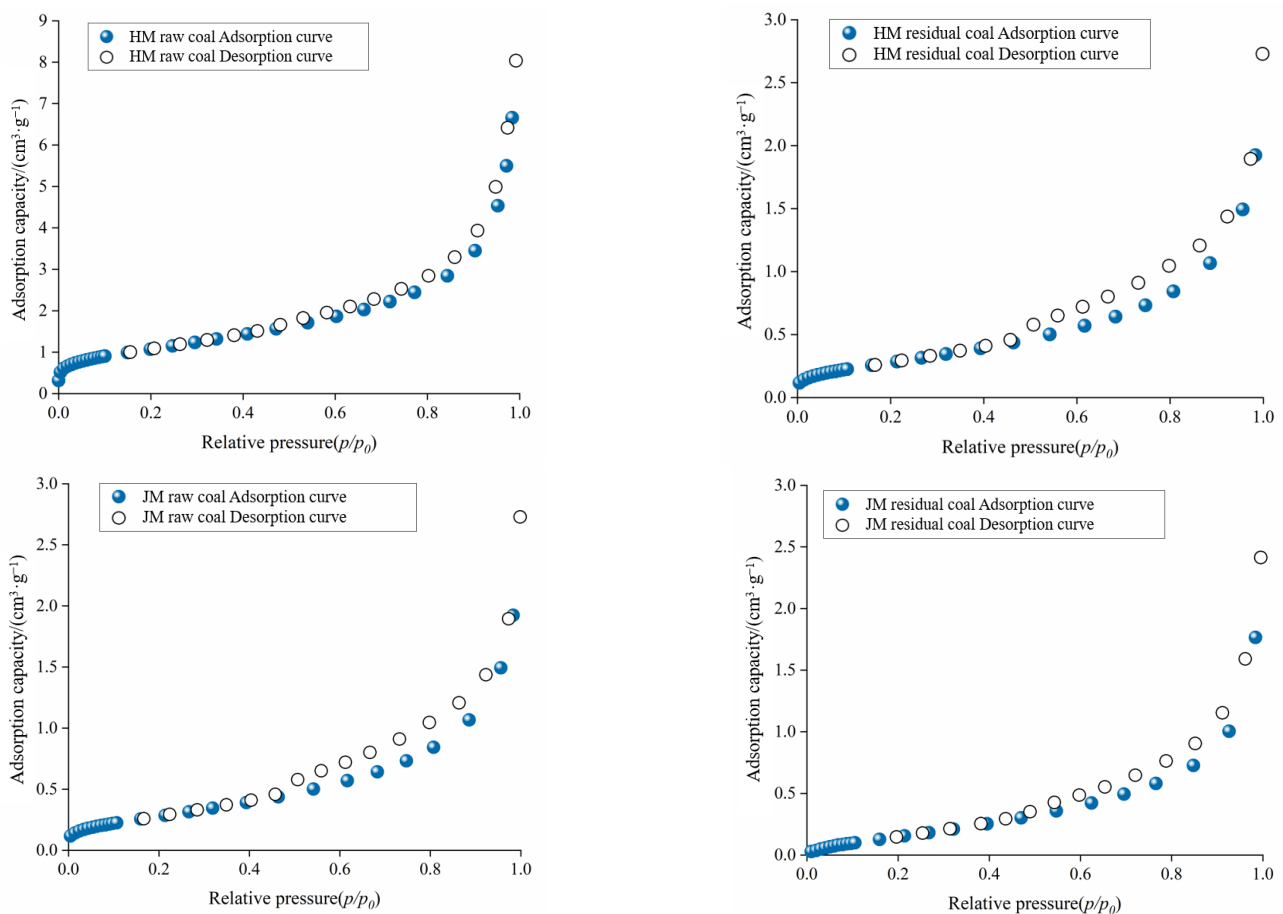


Figure 2. Low-temperature nitrogen adsorption and desorption curves of coal samples.

3.2.2. Variation in the Pore Structure Characteristics of Coal

Various researchers have classified and analyzed the pore space of coal samples. Depending on size, pores were classified as micropores (2–10 nm), transition pores (10–100 nm), mesopores (100–1000 nm) and macropores (>1000 nm) [27]. The properties of coal pores for methane adsorption can be classified as micropores (2–10), transition pores (10–100 nm) and permeable pores (>100 nm) [28]. The four main categories were primary, metamorphic, exogenous and mineral pores according to the pore genesis [29]. The International Union of Pure and Applied Chemistry (IUPAC) currently classifies pore types as micropores (<2 nm), mesopores (2 to 50 nm) and macropores (>50 nm). On balance, the pore size and methane adsorption characteristics of the coal were more suitable for testing the pore characteristics of the coal samples by the mercury-pressure method. The pore genesis classification, on the other hand, was mainly based on sandstone and tuff reservoirs. In this study, the pore types of coal samples were classified based on the IUPAC liquid nitrogen adsorption test. Figure 3 shows the test results. The changes in pore diameter for the HM coal sample were microporous > macroporous > mesoporous, decreasing by 32.48%, 31.07% and 20.22% respectively. The changes in pore size for each JM were microporous > macroporous > mesoporous, with reductions of 51.06%, 4.71% and −1.46%, respectively. There was a correlation between the ability of coal to adsorb methane and its pore structure development [30]. The methane adsorption properties of coal bodies were mainly influenced by a combination of micro- and mesopore distributions, and methane adsorption was mainly concentrated in microporous pores, with mesopores also having an influence [31]. The pore size of HM and JM changed significantly after microbial action.

Because JM was greatly affected by the degree of coalification, the numbers of each pore size were significantly lower than those in HM. The degree of coalification impacts the polycondensation effect in coal samples. The aromatic dense ring system accelerates condensation, and the space between strata becomes smaller, which will significantly reduce the pore size and the number of mesopores. Microorganisms had an obvious effect only on JM micropores, but the number of mesopores increased slightly. The reason for this was that when microorganisms degraded the coal surface, some pores were connected, and micropores were expanded.

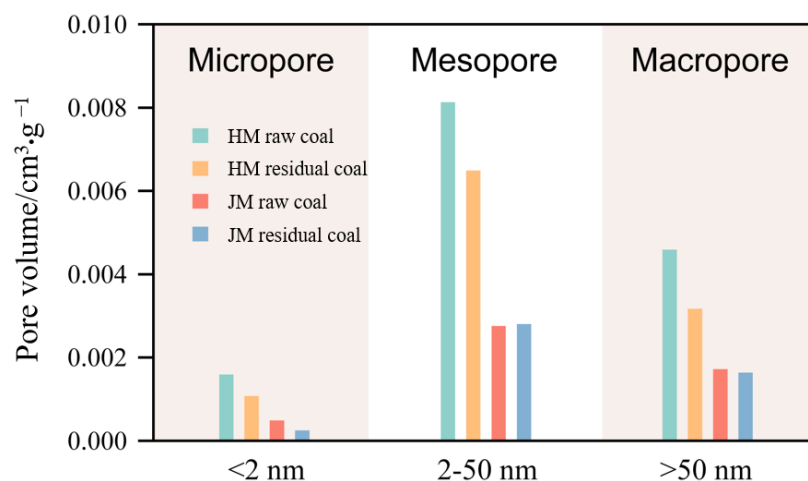


Figure 3. Pore volume of lignite and bituminous coal before and after gas production.

The pores in raw coal have a relatively high specific surface area and micropore volume, which is very beneficial for the storage of coalbed methane but increases the difficulty of coalbed methane development. After microbial degradation, the pore connectivity of the coal reservoir was improved, which was beneficial to coalbed methane enrichment and development.

3.2.3. Variation in the Pore Fractal Characteristics of Coal Reservoirs

Fractal theory is a mathematical method for describing irregularities by means of fractal dimensions. It can be used to study forms or phenomena that have similarities without characteristic lengths and is an important method for quantitatively describing irregularities. The pore structure of coal has non-uniformity and anisotropy. Fractal characteristics can reflect the pore characteristics of coal and characterize the complexity of the coal surface [32]. The fractal dimension is not only a measure of the irregularity of the coal pore structure but is also a parameter that quantitatively describes fractal self-similarity [33]. Many methods exist for calculating the fractal dimension based on the low-temperature liquid nitrogen adsorption experiment, among which the FHH model is the most widely used. The physical properties of the reservoir are positively correlated with the fractal dimension. The main reason for this is that the physical properties of the reservoir are mainly affected by the pore throat size. The adsorption/desorption curve of the coal sample produced a hysteresis loop at a relative pressure of about 0.5, and there was a significant change in the shape and size of corresponding pores before and after the pressure point. Therefore, the FHH model was fitted to two pressure intervals, $P/P_0 < 0.5$ and $P/P_0 > 0.5$, using a relative pressure of 0.5 as the cut-off point. Figure 4 shows the fitted curves. The fractal dimension D1 of the low-pressure section mainly reflects the heterogeneous characteristics of the pore surface. The fractal dimension D2 of the high-pressure section mainly reflects the pore volume and structural heterogeneity. Combined with the results for fractal data (Table 2), the two relative pressures, when segmented, both fit the data well, with correlation coefficients above 0.94; however, the slopes of their fitted straight lines are different, indicating that there are two distinctly different fractal

intervals with different fractal characteristics (D1 and D2). Only the fractal dimension D2 of the HM residual coal showed a slight increase; the rest showed a decreasing trend. The pore structure of the residual coal tended to be generally simpler, with microorganisms dissolving some material on the coal surface, making the surface of the sample smooth; the fractal dimension decreased, and non-homogeneity diminished. As microorganisms degraded and utilized the coal body, microorganisms dissolved some substances on the coal surface. As a result, the coal specific surface area, pore volume and fractal dimension showed an overall decreasing trend, non-homogeneity became worse and the pore size distribution became narrower. The coal surface became smooth, and the complexity of the pore system was weaker. The coal surface reservoir was, thus, modified in the direction of CBM development.

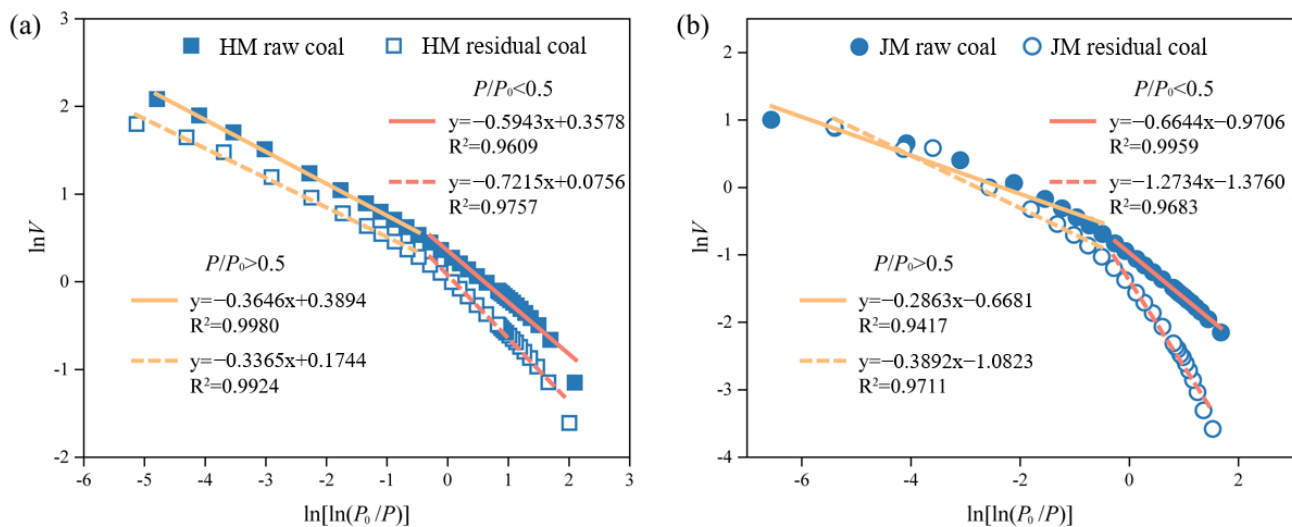


Figure 4. Pore fractal evolution characteristics of coals. (a) Pore fractal evolution characteristics of lignite raw coal and residual coal. (b) Pore fractal evolution characteristics of bituminous raw coal and residual coal.

Table 2. Calculated fractal dimension of adsorption pores based on cryogenic liquid nitrogen adsorption experiments.

Sample Serial Number	$P/P_0 < 0.5$			$P/P_0 > 0.5$		
	A1	D1 = A1 + 3	R2	A2	D2 = A2 + 3	R2
HM-RAW	−0.5943	2.4057	0.9609	−0.3646	2.6354	0.9980
HM-A	−0.7215	2.2785	0.9757	−0.3365	2.6635	0.9924
JM-RAW	−0.6644	2.3356	0.9959	−0.2863	2.7137	0.9417
JM-A	−1.2734	1.7266	0.9683	−0.3892	2.6108	0.9711

As the pore fractal dimension decreased, the coal pore structure became simpler, and the heterogeneity weakened, as shown in Figure 4. The fractal dimension is related to the coal rock composition to some extent. In the early stage of coalification, coal samples were subjected to compaction and dehydration. Water was used to fill in the macropores and mesopores, and the fractal dimension decreased [34]. As the coal metamorphic degree increased, pore dehydration and compaction further intensified; the free water in the pores volatilized, and the pore structure became more complex. Moreover, the middle pores were more likely to be compacted, resulting in micropores and fractures. The ash content of the coal itself also affected the fractal characteristics of the pores to some extent. With a low ash content, mineral particles can fill the pores, enhancing non-homogeneity and reducing the fractal dimension. With a higher ash content, minerals can severely block the pores, increasing the roughness of the coal sample and complicating the pore

structure [35]. Bituminous coal has a large ash content and a significantly lower fractal dimension than lignite.

3.3. Changes in the Adsorption Characteristics of Coal Samples

Methane was mainly desorbed and transported by diffusion within the pore space of the coal. The stronger the coal's ability to adsorb methane, the less diffusible the methane gas becomes, which has a detrimental effect on CBM extraction [36,37]. The adsorption capacity of coal before and after biodegradation was fitted by the Langmuir equation, as shown in Figure 5. The related adsorption parameters of the coal samples are shown in Table 3. The Langmuir volume is usually used to reflect the adsorption capacity of coal to methane. JM is more capable of adsorbing methane than HM. After HM and JM were degraded by microorganisms, the Langmuir volumes decreased by 17.43% and 11.25%, respectively, and the methane desorption efficiency of HM was higher than that of JM. This suggests that the biodegraded coal has a reduced ability to sorb methane, which is related to the reduced number of micropores and mesopores and the fractal dimension of the coal after gas production. The lower the coal rank, the more pronounced the change in the sorption of the coal sample. Isothermal sorption tests demonstrated that the microbial degradation of coal reduces the ability of coal surfaces to sorb methane [38].

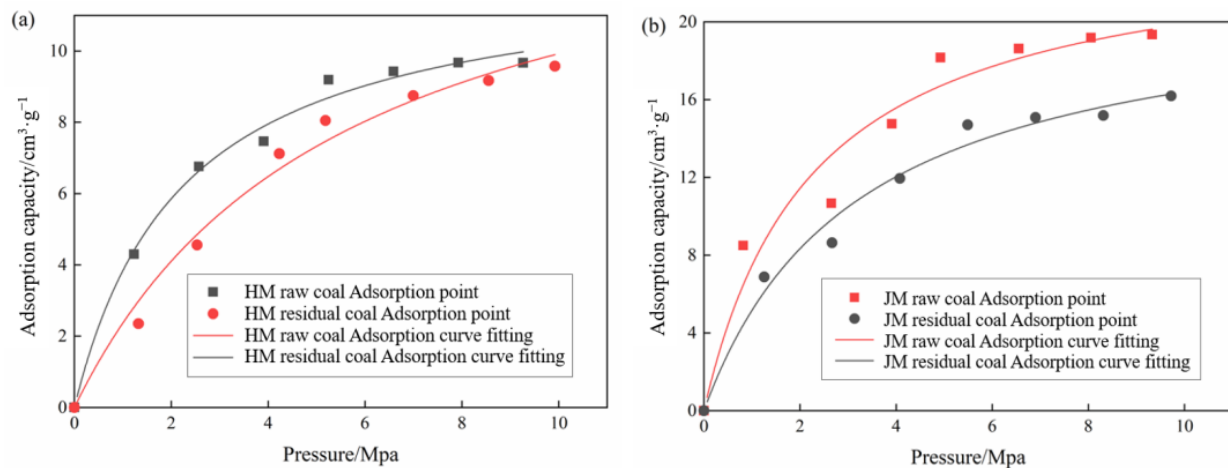


Figure 5. Characteristics of the isothermal curves of coal samples before and after degradation. (a) Adsorption curve of lignite raw coal and residual coal. (b) Adsorption curve of bituminous raw coal and residual coal.

Table 3. Adsorption parameters of coal samples before and after microbial degradation.

Coal	Air Content (m ³ /t)	$V_L/\text{cm}^3 \cdot \text{g}^{-1}$	Rate of Change	P_L/Mpa	P_{cd}/MPa	Goodness of Fit
HM raw coal	5.51	13.722	−17.43%	1.816	1.22	0.9304
HM residual coal		11.330		2.184	2.06	0.9902
JM raw coal	11.8	24.390	−11.25%	2.265	2.12	0.8884
JM residual coal		21.645		3.195	3.83	0.9565

3.4. Variation Characteristics of the Gas Diffusion Coefficient

The gas diffusion coefficient is a key parameter characterizing the degree of diffusion of a gas in coal. By measuring the diffusion of methane gas in coal through a methane diffusion model, the effect of the pore structure on diffusion following the microbial degradation of coal can be investigated. The variation characteristics of the gas diffusion coefficient before and after coal degradation were therefore examined. The peak value of the diffusion coefficient of lignite raw coal was slightly higher than that of bituminous coal, as shown in Figure 6. After microbial degradation, the peak increase in the diffusion coefficient of lignite was much higher than that of bituminous coal. The peak value of

the diffusion coefficient of lignite increased by 48.02%, whereas that of bituminous coal increased by 23.81%. The increase in the gas diffusion coefficient enabled methane gas to escape in large quantities from the coal seam after microbial action, thus increasing the free methane content within the CBM block and achieving an increase in CBM production.

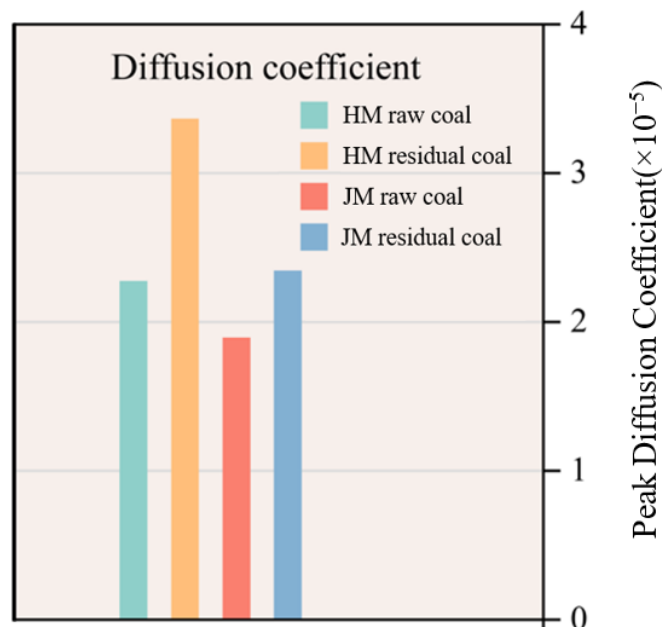


Figure 6. Diffusion coefficient change of pillar coal before and after biodegradation.

3.5. Impact of Microbially Degraded Coal on the Physical Alteration of Coal Reservoirs

In the microbial degradation of methane gas from coal, anaerobic microorganisms degrade the coal structure outside the cell, and it is difficult to easily enter the coal structure. Microorganisms mainly enter the pore structure of coal by secreting extracellular enzymes to produce methane gas. Studies have shown that aerobic microorganisms are more likely to degrade heterocycles in coal, whereas anaerobic microorganisms release extracellular enzymes to produce methane gas. In microbial gas production, the coal itself can be used to limit the production of methane gas, and the later addition of more microbes or nutrients will not produce methane gas. The degree of mutual contact between coal and microorganisms also affects gas production; coal and microorganisms, solids and liquids penetrate and diffuse into each other and complement each other. The physical properties of the coal samples are somewhat different, which can lead to different effects of the microbial production of CBM.

The pore characteristics of coal reflected the degree of contact between coal and microorganisms, and the specific surface area was the indirect expression of the number of microbial adsorption sites. Studies have shown that the more the pores of raw coal expand, the larger their specific surface area is and the more sufficient the contact between the coal and microorganisms is, which is conducive to microbial gas production. Biodegradation can also have an impact on the pore structure of coal. The extracellular enzymes secreted by microorganisms can act on the macromolecular structure of the coal, causing the methoxy and hydroxyl groups attached to the rings of the coal and the volatile substances in the structure of the coal to fall off, followed by the conversion of the free methoxy into methane. Some cocci, bacilli and volatile substances on the coal surface will also block the pore openings, causing both the pore volume and specific surface area of the adsorbed pores in the coal to decrease. This, in turn, weakens the pro-methane capacity of the coal and increases the critical coal desorption pressure, which is manifested in two ways: increased methane production and enhanced desorption capacity. Microbial degradation can improve the porosity and desorption capacity and enhance the diffusion capacity of

methane, thereby improving the physical properties of coal reservoirs and increasing the production of coalbed methane.

The use of microbial degradation to convert some coal into methane gas has not only increased the number of coalbed methane resources but has also changed the physical properties of coal reservoirs. Increasing coal seam solution, permeability and expansion is of great significance to solving the problem of low porosity and low permeability in coal reservoirs and accelerating the industrialization of coalbed methane.

4. Conclusions

- (1) The microbial degradation of coal has an increased biogenic coalbed methane content through the secretion of extracellular enzymes by anaerobic microorganisms. The cumulative gas production of lignite (HM) and bituminous coal (JM) was 152.11 $\mu\text{mol/g}$ and 80.57 $\mu\text{mol/g}$, respectively, and the pore development of the coal itself also affected gas production. Lignite has well-developed pores and a large specific surface area, which facilitate microbial attachment (the secretion of extracellular enzymes) and increase the rate of microbial degradation.
- (2) Microbial action can change the structural characteristics of coal pores, resulting in a decrease in the specific surface area, pore volume and fractal dimension and a tendency for the pore structure of coal to become simpler. The volume of adsorption pores (micropores and mesopores) in coal samples decreased after biodegradation, and methane gas was easily desorbed. After microbial degradation, the pore connectivity of the coal reservoir is improved, which is beneficial to the enrichment and development of coalbed methane.
- (3) Because the metamorphic degree of bituminous coal is higher than that of lignite, the structure of bituminous coal is more difficult to degrade than that of lignite, resulting in a longer hydrolysis stage, and the overall gas production lags behind that of lignite. After microbial degradation, the pore content of each pore diameter of lignite samples decreased, while the micropore effect of bituminous coal was obvious, and the number of mesopores increased slightly. The reason is that lignite is less metamorphic than bituminous coal, and microorganisms are easy to transform it. Compared with lignite, the diffusion coefficient of bituminous coal after microbial degradation increases less, but compared with that before degradation, the diffusion coefficient increases greatly, which can make methane gas escape in a large amount in the coal seam after microbial transformation so as to achieve the effect of increasing coalbed methane production.
- (4) Microbial degradation has a large impact on the physical properties of coal reservoirs, which not only increases the extractable CBM content but also increases the critical desorption pressure, improving the CBM desorption–diffusion transport capacity and realizing the CBM dual-production enhancement effect.

Author Contributions: Conceptualization, D.X. and, Z.C.; methodology, D.X.; software, P.G.; validation, P.G., L.C. and, S.C.; formal analysis, G.W.; investigation, Z.W.; resources, Z.C.; data curation, D.X.; writing—original draft preparation, P.G.; writing—review and editing, D.X.; visualization, Z.W.; supervision, Y.Z.; project administration, D.X.; funding acquisition, Z.C. All authors have read and agreed to the published version of the manuscript.

Funding: This research was funded by the National Natural Science Foundation of China (41972178, 42072193), the Outstanding Youth Science Foundation of Henan Province (202300410168) and the Young Backbone Teacher Foundation of Henan Province (2018GGJS059).

Data Availability Statement: The datasets used and/or analyzed during the current study are available from the corresponding author on reasonable request.

Acknowledgments: This work was supported by the National Natural Science Foundation of China (41972178, 42072193), the Outstanding Youth Science Foundation of Henan Province (202300410168) and the Young Backbone Teacher Foundation of Henan Province (2018GGJS059).

Conflicts of Interest: The authors declare no conflict of interest.

References

1. Cao, M.L.; Kang, Y.S.; Qin, S.F.; Zhang, B.; Deng, Z. Single-factor physical simulation experiment study on matrix contraction effect of coal rocks with different ranks. *J. China Coal Soc.* **2021**, *46*, 364–376.
2. Lu, Y.Y.; Chai, C.J.; Zhou, Z.; Ge, Z.L.; Yang, M.M. Influence of bioconversion on pore permeability of coal seams. *J. Min. Saf. Eng.* **2021**, *38*, 165–172.
3. Cheng, Y.P.; Lei, Y. Causality between tectonic coal and coal and gas outbursts. *J. China Coal Soc.* **2021**, *46*, 180–198.
4. Dong, X.X.; Li, W.J.; Liu, Q.; Wang, H.H. Research on convection-reaction-diffusion model of contaminants in fracturing flowback fluid in non-equidistant fractures with arbitrary inclination of shale gas development. *J. Pet. Sci. Eng.* **2022**, *208*, 109479. [[CrossRef](#)]
5. Liu, X.Q.; Sun, Y.; Guo, T.K.; Rabiei, M.; Qu, Z.Q.; Hou, J. Numerical simulations of hydraulic fracturing in methane hydrate reservoirs based on the coupled thermo-hydrologic-mechanical-damage (THMD) model. *Energy* **2022**, *238*, 122054. [[CrossRef](#)]
6. Duplyakov, V.M.; Morozov, A.D.; Shel, E.V.; Vainshtein, A.L.; Burnaev, E.; Osiptsov, A.A.; Paderin, G.V. Data-driven model for hydraulic fracturing design optimization. Part II: Inverse problem. *J. Pet. Sci. Eng.* **2022**, *208*, 109603. [[CrossRef](#)]
7. Liu, Y.L.; Tang, D.Z.; Xu, H.; Zhao, T.T.; Hou, W. Effect of interlayer mechanical properties on initiation and propagation of hydraulic fracturing in laminated coal reservoirs. *J. Pet. Sci. Eng.* **2021**, *3*, 109381. [[CrossRef](#)]
8. Tian, W. Study on the Existing State of CO₂ in Geological Storage of old Oilfields. *Chin. J. Undergr. Space Eng.* **2021**, *17*, 618–625.
9. Gong, H.R.; Wang, K.; Wang, G.D.; Yang, X.; Du, F. Underground coal seam gas displacement by injecting nitrogen: Field test and effect prediction. *Fuel* **2021**, *306*, 121646. [[CrossRef](#)]
10. Cai, M.Y.; Su, Y.L.; Hao, Y.M.; Guo, Y.C.; Elsworth, D.; Li, L.; Li, D.S.; Li, X.Y. Monitoring oil displacement and CO₂ trapping in low-permeability media using NMR: A comparison of miscible and immiscible flooding. *Fuel* **2021**, *305*, 121606. [[CrossRef](#)]
11. Xiong, C.M.; Li, S.J.; Ding, B.; Geng, X.F.; Zhang, J.; Yan, Y.G. Molecular insight into the oil displacement mechanism of gas flooding in deep oil reservoir. *Chem. Phys. Lett.* **2021**, *783*, 139044. [[CrossRef](#)]
12. Song, Y.; Zhao, C.; Chen, M.; Chi, Y.; Zhang, Y.; Zhao, J.F. Pore-scale visualization study on CO₂ displacement of brine in micromodels with circular and square cross sections. *Int. J. Greenh. Gas Control* **2020**, *95*, 102958. [[CrossRef](#)]
13. Wang, S.J.; Jiang, L.L.; Cheng, Z.C.; Liu, Y.; Zhao, J.F.; Song, Y.C. Experimental study on the CO₂-decane displacement front behavior in high permeability sand evaluated by magnetic resonance imaging. *Energy* **2021**, *217*, 119433. [[CrossRef](#)]
14. Wang, Q.; Yang, S.L.; Bai, J.; Zhao, W.; Li, J.J.; Chen, H. Influence of pore throat structure on changes in physical properties of reservoir rock during CO₂ flooding. *Acta Pet. Sin.* **2021**, *42*, 654.
15. Li, Y.; Wang, Y.; Wang, Z.S.; Pan, Z.J. Variation in permeability during CO₂-CH₄ displacement in coal seams: Part 1—Experimental insights. *Fuel* **2020**, *263*, 1–10. [[CrossRef](#)]
16. Yu, M.H.; Song, Y.C. CO₂/Water Displacement in Porous Medium Under Pressure and Temperature Conditions for Geological Storage. *Energy Procedia* **2014**, *61*, 282–285. [[CrossRef](#)]
17. Zhi, S.; Elsworth, D.; Wang, J.H.; Gan, Q.; Liu, S.M. Hydraulic fracturing for improved nutrient delivery in microbially-enhanced coalbed-methane (MECBM) production. *J. Nat. Gas Sci. Eng.* **2018**, *60*, 294–311. [[CrossRef](#)]
18. Scott, A. Improving Coal Gas Recovery with Microbially Enhanced Coalbed Methane. In *Coalbed Methane: Scientific, Environmental and Economic Evaluation*; Springer: Berlin/Heidelberg, Germany, 1999.
19. Xiao, D.; Peng, S.P.; Wang, E.Y. Fermentation Enhancement of Methanogenic Archaea Consortia from an Illinois Basin Coalbed via DOL Emulsion Nutrition. *Plos ONE* **2015**, *10*, eO124389. [[CrossRef](#)]
20. Hou, D.S.; Liang, W.G.; Zhang, B.N.; Li, C. Seepage law of mixed gases in CO₂ displacement of coal seam CH₄. *J. China Coal Soc.* **2019**, *44*, 3463–3471.
21. Pandey, R.; Harpalani, S.; Feng, R.M.; Zhang, J.; Liang, Y.N. Changes in gas storage and transport properties of coal as a result of enhanced microbial methane generation. *Fuel* **2016**, *179*, 114–123. [[CrossRef](#)]
22. Wang, X.; Cheng, Y.; Zhang, D.; Liu, Z.D.; Wang, Z.Y.; Jiang, Z.G. Influence of tectonic evolution on pore structure and fractal characteristics of coal by low pressure gas adsorption. *J. Nat. Gas Sci. Eng.* **2021**, *35*, 3887–3898. [[CrossRef](#)]
23. Huang, H.P.; Eric, W. A laboratory investigation of the impact of solvent treatment on the permeability of bituminous coal from Western Canada with a focus on microbial in-situ processing of coals. *Energy* **2020**, *210*, 118542. [[CrossRef](#)]
24. Xia, D.P.; Huang, S.; Yan, X.T. Influencing mechanism of Fe²⁺ on biomethane production from coal. *J. Nat. Gas Sci. Eng.* **2021**, *91*, 103959. [[CrossRef](#)]
25. Chen, Y.; Ma, Z.Y.; Ma, D.M.; Li, W.B.; Li, G.F.; Yang, F.; Zheng, C.; Teng, J.X.; Ji, Y.S. Effects of wettability differences of different macroscopic composition of coal on methane adsorption and desorption. *Coal Sci. Technol.* **2021**, *49*, 47–55.
26. Li, S.G.; Bai, Y.; Lin, H.F.; Yan, M.; Long, H.; Guo, D.D. Effect of N₂/CO₂ injection pressure on CH₄ desorption in gas-bearing coal rock. *Nat. Gas Ind.* **2021**, *41*, 80–89.
27. Zdravkov, B.D.; Cermak, J.J.; Martin, S. Pore classification in the characterization of porous materials: A perspective. *Cent. Eur. J. Chem.* **2007**, *5*, 385–395.
28. Qin, Y.; Xu, Z.W.; Zhang, J. Natural classification of the high-rank coal pore structure and its application. *J. China Coal Soc.* **1995**, *3*, 266–271.
29. Zhang, H. Genetical type of proes in coal reservoir and its research significance. *J. China Coal. Soc.* **2001**, *1*, 40–44.
30. Cheng, G.; Jiang, B.; Li, M.; Zeng, F.G.; Xiang, J.H. Effects of pore-fracture structure of ductile tectonically deformed coals on their permeability: An experimental study based on raw coal cores. *J. Pet. Sci. Eng.* **2020**, *193*, 107371. [[CrossRef](#)]

31. Shen, J.; Qin, Y.; Li, Y. Experimental investigation into the relative permeability of gas and water in low-rank coal. *J. Pet. Sci. Eng.* **2019**, *175*, 303–316. [[CrossRef](#)]
32. Sun, Y.F.; Zhao, Y.X.; Wang, X.; Peng, L.; Sun, Q. Synchrotron radiation facility-based quantitative evaluation of pore structure heterogeneity and anisotropy in coal. *J. Books* **2019**, *46*, 1195–1205. [[CrossRef](#)]
33. Liu, K.; Ostadhassan, M.; Jang, H.W.; Zakharova, N.V.; Shokouhimehr, M. Comparison of fractal dimensions from nitrogen adsorption data in shale via different models. *RSC Adv.* **2021**, *11*, 2298–2306. [[CrossRef](#)] [[PubMed](#)]
34. Zhu, H.J.; Ju, Y.W.; Qi, Y.; Huang, C.; Zhang, L. Impact of tectonism on pore type and pore structure evolution in organic-rich shale: Implications for gas storage and migration pathways in naturally deformed rocks. *Fuel* **2018**, *228*, 272–289. [[CrossRef](#)]
35. Urai, S.; Desbois, G.; Urai, J.L.; Schroppel, B.; Schwarz, J.O. Multi-scale characterization of porosity in Boom Clay (HADES-level, Mol, Belgium) using a combination of X-ray μ -CT, 2D BIB-SEM and FIB-SEM tomography. *Microporous Mesoporous Mater. Off. J. Int. Zeolite Assoc.* **2015**, *208*, 1–20.
36. Han, W.C.; Li, A.F.; Fang, Q. Comparative analysis of isothermal adsorption models for coals with water content under supercritical conditions. *J. China Coal Soc.* **2020**, *45*, 4095–4103.
37. Yang, Y.; Liu, S.M.; Liu, W.; Wang, L. Intrinsic relationship between Langmuir sorption volume and pressure for coal: Experimental and thermodynamic modeling study. *Fuel* **2019**, *241*, 105–117. [[CrossRef](#)]
38. Zheng, Y.F.; Zhai, C.; Sun, Y.; Xu, J.Z.; Cong, Y.Z.; Tang, W.; Chen, A.K. Experimental study on the effect of coal particle size on the mechanics, pore structure, and permeability of coal-like materials for low-rank coalbed methane reservoir simulation. *Energy Fuels* **2021**, *35*, 17566–17579. [[CrossRef](#)]

Disclaimer/Publisher’s Note: The statements, opinions and data contained in all publications are solely those of the individual author(s) and contributor(s) and not of MDPI and/or the editor(s). MDPI and/or the editor(s) disclaim responsibility for any injury to people or property resulting from any ideas, methods, instructions or products referred to in the content.